Time series of flood mapping in the Mekong Delta using high resolution satellite images

Time series of flood mapping in the Mekong Delta using high resolution satellite images

D A Dinh[1,2], B Elmahrad[1,3], P Leinenkugel[2] and A Newton[1]

[1] CIMA, FCT-Gambelas Campus, University of Algarve, 8005-139 Faro, Portugal
[2] German Remote Sensing Data Center (DFD), Earth Observation Center (EOC), Aerospace Center (DLR), Oberpfaffenhofen, Wessling, Germany
[3] Department of Earth Sciences, CERN2D, Faculty of Sciences, Mohamed V University, Rabat, Morocco

E-mail: dinhdieuanh1319@gmail.com

Abstract. The Mekong Delta, located in Southern Vietnam, is one of the most affected areas in the world by climate change and sea level rises, especially flooding. Therefore, flood mapping is essential for understanding the flood regime and mitigating its impacts. Remote sensing and GIS can support the accurate and area wide evaluation of floods. In this study, high spatial resolution synthetic aperture radar (SAR) and optical data were used to generate a dense satellite data time series for analysing the spatio-temporal patterns of flooding in the Mekong Delta. To derive water masks, a total of 777 Sentinel-1, 515 Sentinel-2 and 57 Landsat-8 scenes were used to generate cloud free water masks at a 10m spatial resolution in regular 10-day intervals throughout the observation period of hydrological years 2016-2017. The results show a spatial explicit information on the core zones of the seasonal flooding processes for the entire Mekong Delta and their effect of using floodwater for rice cultivation. The outcome maps provide an overall understanding of Mekong Delta flood patterns and many valuable information for policymakers and water resources managers.

1. Introduction

A flood occurs when excess water upstream flows over river banks or dikes to the floodplain, especially, when the water flow submerges area that is generally dry. Inundation is affected by floods. Flood water may be freshwater from upstream or/and saltwater from the sea due to the tide [1]. Flooding has severe economic and social impacts [2]–[4]. However, it has also environmental and socio-economic benefits [5] such as the annual flooding which is also called “beautiful” flood supplied freshwater for irrigation and domestic use [6], increased fishery resources [7], improved navigation transport, brought about more natural fertilizer, flushed contaminated water caused by sulfate soils and transported salted water towards the sea such as the case of South China Sea [8].

Flooding is increasing in frequency and magnitude along with sea level rise, seasonal tropical storms and high tides in the Mekong Delta [1]. The Mekong Delta has been identified as one of the most sensitive and exposed regions to climate change and sea level rise phenomena [8]. In the official climate change and sea level rise report by the Ministry of Natural Resources and Environment, it is estimated that 21%, 28.2% and 38.9% of the Mekong Delta area will be flooded if the sea level increases by 80cm, 90cm and 100cm respectively [9]. Floods often impact large regions, which are difficult to access from

the ground [10]. Therefore, earth observation technologies are expected to provide powerful techniques for detecting flooded areas [11], [12].

There are numerous studies about flood mapping and monitoring with SAR data based on sensors such as ERS-1/2, ENVISAT ASAR, RADARSAT, TerraSAR-X [13]–[18]. Many studies were conducted on mapping the flood events in the Mekong Delta using remote sensing [11], [19]–[22]. MODIS data at 500m resolution was often used for mapping flood in this region [21]. Envisat ASAR WSM data at 150m resolution was used to analyze flood in Mekong delta between 2007 and 2011 and was difficult to detect flooded areas beneath dense tree cover and was limited by insufficient data availability for true time series analysis [20]. Even though these studies, there is still limited research on flood mapping using high spatial and temporal resolution in the Mekong Delta [23], [24], especially in larger time series.

In order to ensure high temporal and spatial resolution for flood mapping there is a need of using and combining data sets from different sensors. This study aims to generate flood mapping based on SAR and optical data with high temporal and spatial resolution which enhances flood monitoring by proposing a new way to efficiently process SAR data. In addition, the flooding patterns and frequency were conducted and their attribution of the trends to land use land cover (LULC). This study proposes solutions for decision-making and water resources management planning.

2. Study areas

The Mekong Delta, located in southern Vietnam with an area of 39,000 km^2 between latitude 8°30′ - 11°30′ N and longitude 104°30′ -106°50′ E [20], usually people call it “Vietnam's Rice Bowl” and the full “fish basket” of the country [8], as it’s land known by a large rice production [23] and aquaculture areas. It begins near Phnom Penh and ends up as a huge fertile flat plain in southern Vietnam where the largest tributary, the Bassac River, branches away from the Mekong River (Fig.1). The delta is a home to over 17.6 million inhabitants, spreading in 13 provinces and cities with an intensity of 432 people per square kilometer [25]. It has two main rivers (Mekong and Bassac) which splits into a number of smaller distributaries, forming an area known as the Nine Dragons [26]. It has the longest river in Southeast Asia, the Vietnamese Mekong River Delta (VMD) which runs 4,800 km through China, Myanmar, Thailand, Laos, Cambodia, and then forms a delta in Vietnam before entering the sea. VMD is a watery land- scape consisting of Mekong’s two main distributaries and a dense network of numerous natural and artificial channels (Fig. 1). It contributes to 75% of Vietnam’s total agricultural-fishery-forestry production, over 50% of agricultural exports, and 90% of rice exports [27].

Mekong Delta is a coastal floodplain that is subjected to natural hazards such as floods, droughts and saltwater intrusion, which destroy rice crops and impact farmer livelihoods and food security.

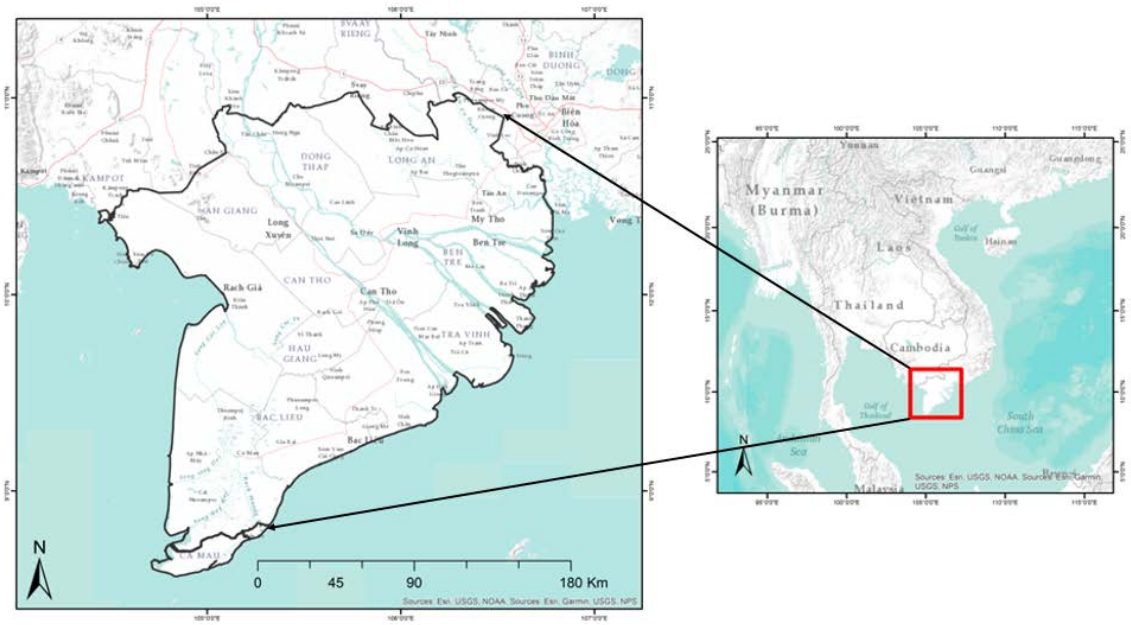

Figure 1. Mekong Delta

3. Materials

In this paper we used Synthetic Aperture Radar (SAR) data (Sentinal-1) and optical data (Sentinal-2, Landsat 8 and MODIS).

As main data source, we used a 5m*20m resolution Sentinel-1, Level-1 Ground Range Detected (GRD) images in Interferometric Wide Swath (IW) mode resampled to 10m pixel spacing. In total 777 Sentinel-1 GRD-IW data in VH and VV polarization were acquired over the Mekong Delta. From these, 705 scenes originate from Sentinel-1A acquired from January 1, 2016 to October 3, 2017 and 72 scenes originating from Sentinel-1B acquired from June 27, 2016 to September 26, 2017.

Since Sentinel-1 could not provide sufficient data coverage, we used Sentinel-2 Multi-Spectral Imager (MSI) data to fill the gaps. In total 515 Sentinel 2 MSI scenes with 10-meter spatial resolution were acquired from January 1, 2016 to September 27, 2017 using the Google Earth Engine tool. Each Sentinel-2 scene contains 13 spectral bands representing Top of Atmosphere (TOA) reflectance scaled by 10000. The spectral bands used in this study were Band-2 (490 nm/blue), Band-3 (560 nm/green), Band-4(665 nm/red) and Band-8 (842 nm/ near Infrared).

Furthermore, Landsat-8 data at a 30-meter spatial resolution were acquired from January 1, 2016 to March 11, 2017 using Google Earth Engine and which contains 7 bands, cloud mask (cfmask) and cloud mask confidence (cfmask_conf). There were 57 Landsat-8 scenes achieved from these dates.

While with Sentinel-1, Sentinel-2 and Landsat-8 data regular flood maps could be produced in regular intervals, in some rare cases data gaps remained for some spatially limited areas. For these cases, information on flooding state was retrieved from the DLR Global Water Pack which is a globally available daily flood information product developed on the basis of the MODIS sensor which provides daily global coverage which is particularly useful for continental to global scale assessments and for assessing rapidly changing surface properties.

4. Methods

The DLR Wamapro software was used for deriving water masks based on Sentinel-1 SAR data. The software is a license-free tool and can be applied to data from all available SAR sensors. It use a simple pixel-based thresholding method, which allows the separation of water pixels from non-water pixels, characterized by very low and higher backscatter values in the image histogram, respectively. Ten backscatter thresholds for land and water areas were tested to detect water bodies in the Mekong Delta

and Tonle Sap region of Southern Vietnam. The thresholds were adapted estimates from standard thresholds used in the Wamapro Tool (water= -2200, land= -1600). After applying the different threshold pairs the results were visually interpreted and evaluated. Tested thresholds were applied to a corresponding image to classify it into two classes of water and non-water (land) respectively. The water pixels coded as '1' while the non-water pixels coded as '0'. The year 2016 was chosen for threshold testing. For each month in 2016 one Sentinel-1 dataset was chosen to test all 10 threshold combinations to evaluate if seasonal water properties result in threshold differences, and if the thresholds differ for different satellite over paths. 12 seasonal scenes were chosen spatially randomly from the Mekong Delta area, scenes far North of Tonle Sap were excluded so far. All threshold combinations were compared pairwise. Thereby the winning threshold was kept and compared to a new threshold pair in the list. Finally, the threshold Wt= -2000; Lt= -1600 was chosen to be the winning threshold combination since it produced the most accurate results, even for small water bodies. Subsequently all 777 SAR scenes were processed by applying this water threshold.

On the basis of the 777 water masks from Sentinel-1, high spatial resolution water mask composites were generated for different temporal intervals, i.e. 5-day, 10-day, 20-day, and 30-day intervals. Therefore, the observation period from January 1, 2016 to September 26, 2017 was divided into 5-, 10-, 20-, or 30-day intervals and all images with acquisition dates lying within a respective interval were combined to one mosaic image using ArcGIS. Each temporal water mask composites potentially could have three classes which are 0=land, 1=water and 255=No data.

The Sentinel-2 MSI and Landsat-8 data processing was conducted in Google Earth Engine (GEE). In total 515 Sentinel-2 images were processed to a total of 44 10-day composites using the same method as described for Sentinel-1 data. In total 57 Landsat water masks were mosaicked with Sentinel-1 and Sentinel-2 to 10-days composites. The composites have three classes which are 0=land, 1=water and 255=No data. The final composite was combined by Sentinel-1 data from the DLR Global Water Pack and Sentinel-2, Landsat-8 data, using ArcGIS 10.3.1 software. To investigate the floodwaters impacts on LULC in the Mekong Delta, Microsoft Excel was used.

5. Results and discussion

5.1. Spatial-temporal flood patterns

Figure 2 shows the flooding regime for the Mekong Delta during the rainy season within the hydrological year 2016-2017, which begins in July until the end of June. It can be seen that the water begins to spread over the northern floodplains of the Mekong Delta coming from the Tonle Sap Lake in Cambodia. In the year 2016, flood happened in the north and the south-west of the Mekong Delta. The floodwaters started to increase in July at a rising stage, where water growth from north to south. According to Kuenzer et al., 2013 [20], the main causes of inundation spread in the Mekong Delta are river-induced and overland flow. The flooding continued to rise over August-September and peaked in October. The high stage of flooding was during October and November. From the end of November, floodwater retreated back from south to north which was further from the river branches' areas. Nevertheless, floodwaters abruptly increased again in March and May 2017 which is related to the controlled irrigation in the course of rice paddy cultivation in combination with heavy rain during this period. The floodwaters declined in June 2017. As measured at in situ gauge stations at the northern border, the flood peaks of the Mekong Delta are between mid-July to mid-August and between September and October [28].

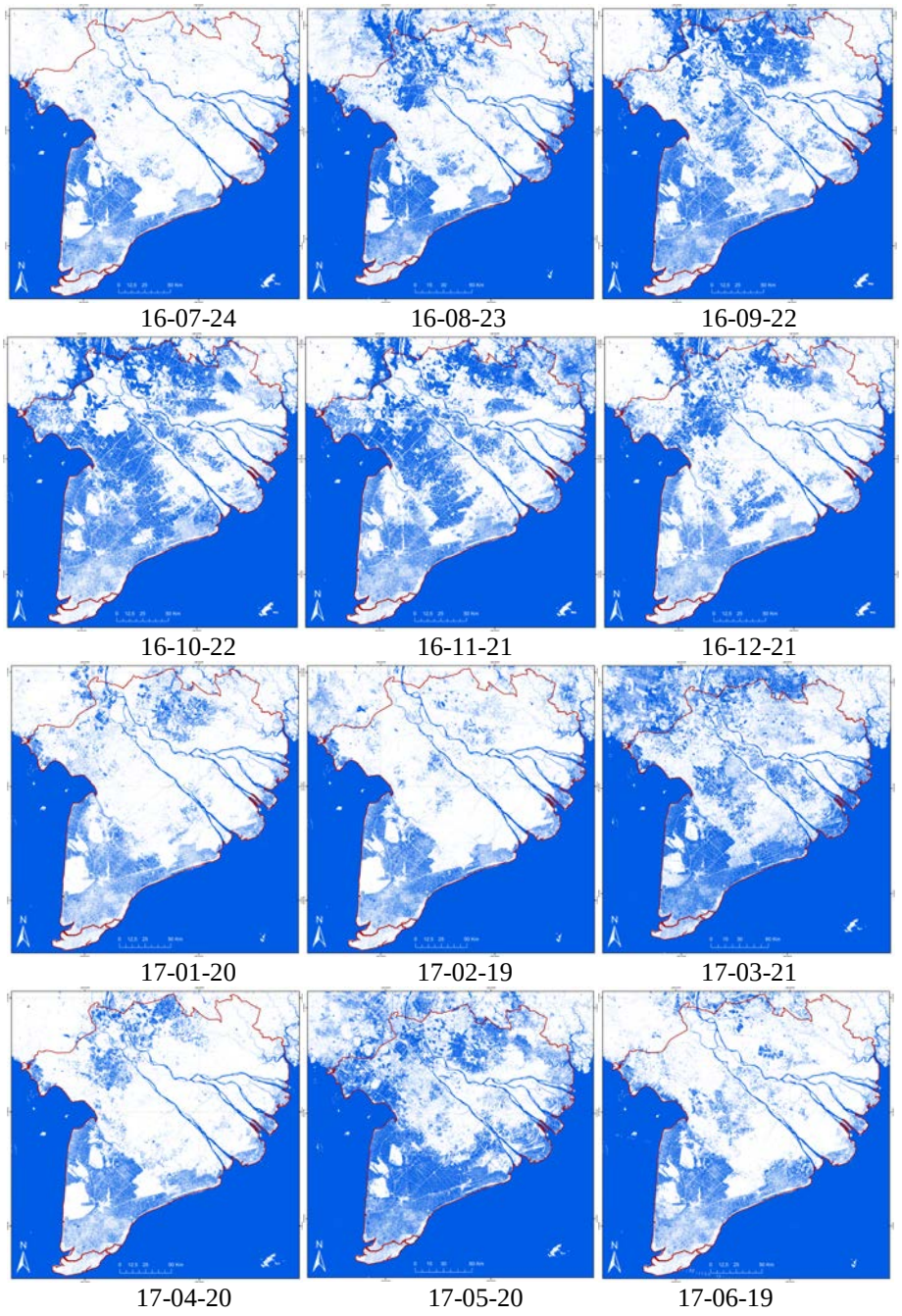

Figure 2. Flooding patterns in the hydrological year 2016/2017

The line graph in figure 3 also depicts the spatio-temporal pattern of the seasonal flooding in the Mekong Delta over the hydrological year 2016-2017. The y-axis shows the percentage of water area derived from each 10-day composite from July 4, 2016 to June 29, 2017. As it can be seen, the water area began to increase with the start of the flood season in July with an initial percentage of 15% water area. The floodwater increased gradually in August-September with 25-30% of water area. The high flood occurred in the middle of October with the peak of 46%. The floodwater decreased and remained at over 20% in November-December. During January-February, the water areas fluctuated around 15% and rose approximately 30% in mid-March. Floodwaters declined at the end of March to 20%. The same

flooding patterns happened in April. At the end of April, it started to increase and remained roughly 35% until May. The flood areas dropped in June with 15% of water area.

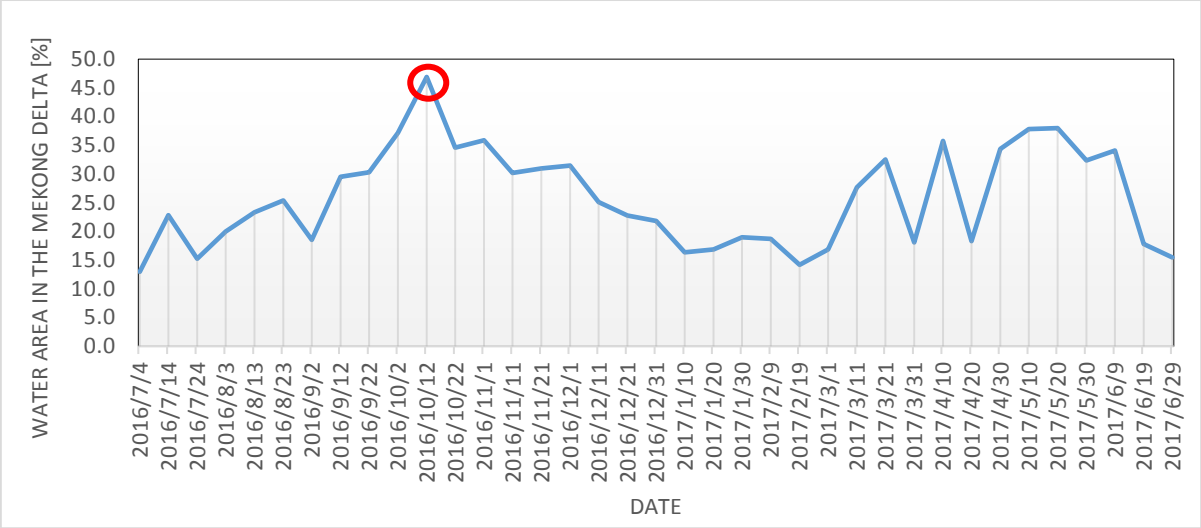

Figure 3. Flooding patterns in the hydrological year 2016/2017

5.2. Flooding patterns in relation to land use land cover in the Mekong Delta

Due to the strong relationship between agricultural land use and flood patterns in the Mekong Delta in this paragraph more details on the spatial-temporal flooding patterns on rice cultivation are provided and discussed. The growing seasons in the Mekong Delta, include the winter-spring (WS) season (November-December to March-April), the spring-summer (SS) season (March-April to June-July), the summer-autumn (SA) season (April-May to July-August) and the autumn-winter (AW) season (August-September to November-December). According to Vietnam General Statistics Office, there are three main rice-cropping systems: single-season rice crops, double season rice crops and triple season rice crops [29].

Figure 4 shows the flooding pattern for the single-season rice-shrimp crops aggregated overall sample areas. The percentage of water was more than 90% from March to August for the period of 2016-2017. The water is pumped out of the floodplain compartments in January 2016. During the growing stage between October and February water is nearly absent. After this period, the water began to increase from February (48%) in October (74%). The water remained high at around 90% for 8 months then declined to 12% in November. The water percentage rose from 26.78% in January to 94.42% in March 2017. The peak was 99.22% in July. Afterward, it reduced to 60.89% in September. The single-season rice-shrimp cropping system depends on the salinity and the beginning of the rainy season time. In addition, the single rice-shrimp crops are near the coastlines. After harvesting shrimp in the middle of September, the rice was sowed. Those are the reasons why the percentage of water was always high from March to September.

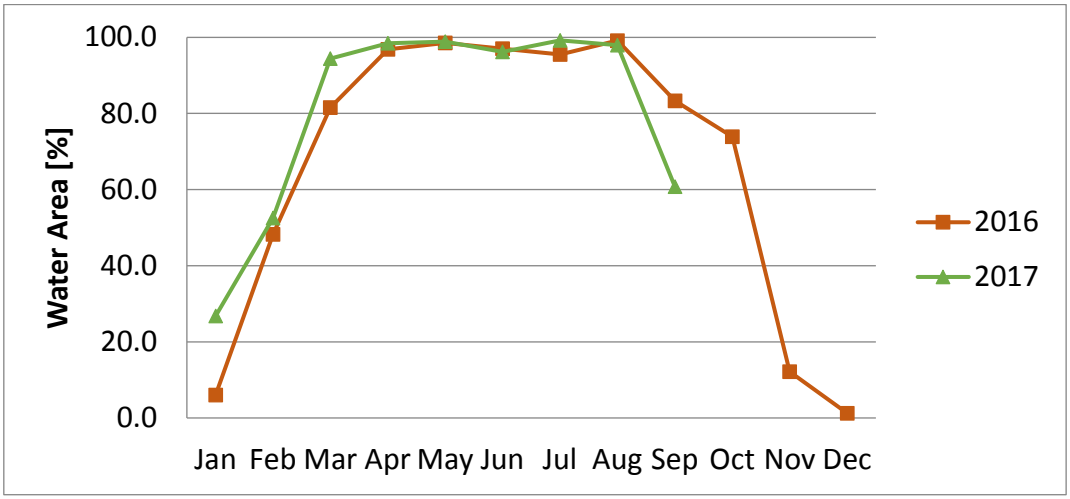

Figure 4. Flooding Patterns for Single Season Rice-Shrimp Crops

The flooding pattern for double season rice crops in the summer-autumn and autumn-winter growing seasons is shown in Figure 5. There are two flood cycles from April to July and October to December in the growing season each year. Rice fields are usually flooded prior to transplanting rice seedlings from a nursery into the fields. Therefore the flood peaks can be usually found in June and November while the lowest water percentage can be found around February and September. In 2016 there were slight differences in the temporal pattern resulting in earlier flooding and two peaks in April and June within the first season. The 2017 flooding pattern shows a distinct peak in May and November with about 70% of the samples flooded during this time. This double season rice cropping system (SA-AW) is located in the coastline areas and harvested in the middle September for SA growing season and in January for AW growing season.

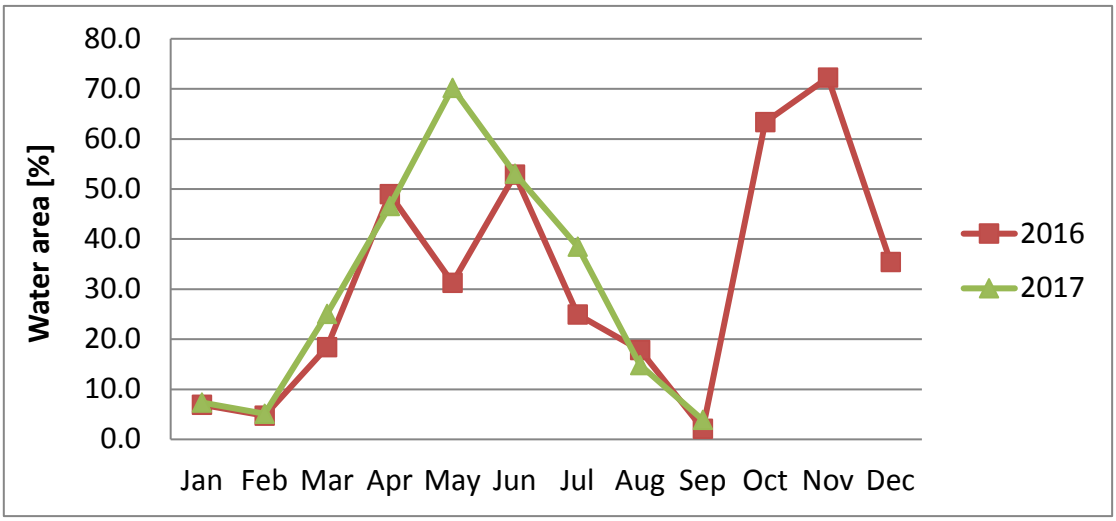

Figure 5. Flooding Patterns for Double Season Rice Crops (SA-AW)

The flooding patterns for the double season rice crops in the winter-spring and summer-autumn growing season is shown in Figure 6. In the aggregated statistics for 2016 and 2017, there were two cycles of flooding can be identified which took place in April-May (77%) and July-September (97%). In 2016 there was a smaller flooding peak around March with a larger flooding cycle from July to December.

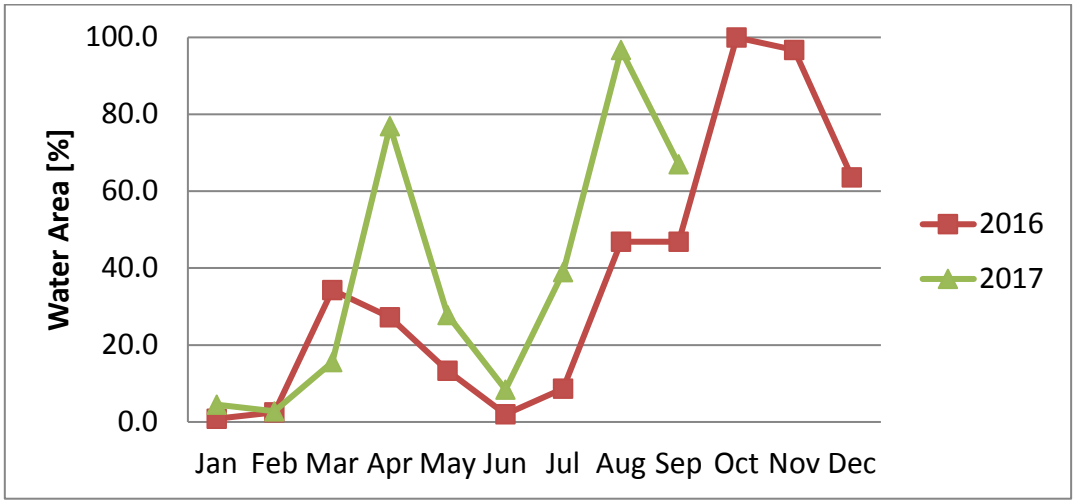

Figure 6. Flooding Patterns for Double Season Rice Crops (WS-SA)

Figure 7 shows the flooding patterns for triple season rice crops. There were three flood cycles each year except for 2017 since for 2017 the data coverage only lasts until September. Flooding peaks were between April-May, August, and December. It can be seen that compared to the single cropped rice paddy (figure 4) the double- and triple-cropped rice areas have a short first growing season typically below 80 days. For triple-crop schemes, the second season is short as well, whereas double crop exhibits a longer second season.

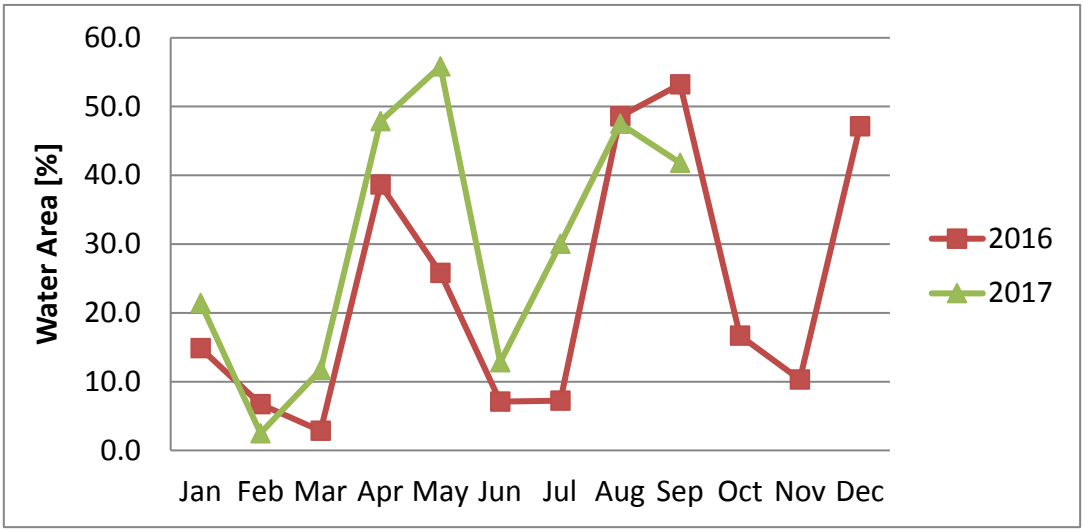

Figure 7. Flooding Patterns for Triple Season Rice Crops

6. Conclusion

There are multiple flooding periods within each year related on the one hand to the natural hydrological cycle of the Mekong River and on the other hand related to the cultivation schemes of the rice farmers. In the hydrological year 2016/2017, the floodwater rose constantly in August to September with 25-30% of the area under water. During the flood peak, nearly half of the Mekong Delta (46%) was covered by water in the middle of October. The areas most affected by inundation are northern and southwestern of the Mekong Delta. Particularly the provinces An Giang, Dong Thap, Long An, Kien Giang and Can Tho are those most impacted by flooding. The southern coastal provinces and the south-eastern regions are less affected by flooding because the flooding emanates from the main branches of the Mekong spreading over the low lying flood plains further inland and not from e.g. storm surges along the coast.

As could be shown in large areas of the Mekong Delta the flood patterns are predominantly the result of controlled flooding in the course of agricultural cultivation, predominantly rice paddy or from aquaculture. The farmers use the flood water during the transplanting phase of rice and after several weeks the water is pumped out again. The period of flooding differs and depends also on the number of growing seasons. The areas where a triple rice crop is possible are distributed mainly in the upper part of the Mekong Delta, behind the full-dike system. The double rice crops areas are also located in the upper and middle part of the Mekong Delta, behind the semi-dike system. Flooding frequency is greater in the double rice crop areas than the triple rice crop areas. Furthermore, particularly in the southern coastal provinces such as Ca Mau, large extents are flooded permanently related to aquaculture cultivation.

Combining current high spatial resolution Sentinel sensors from the Copernicus program can provide a satellite data time series with satisfying temporal intervals at an outstanding spatial resolution of 10m. While 10-day intervals are not sufficient for near-real time monitoring, they provide enough information to monitor fast changing processes such as flooding and water usage for rice cultivation at the field level. Furthermore, the monitoring at regular interval allows for quantitative and comparative intra- and inter-annual analyses of flood dynamics. The SAR satellite Sentinel-1 is the most important data source, particularly in cloud prone regions, since it provides clear and undistorted data even in periods of dense cloud cover. In addition, water areas can be clearly identified in SAR data as a result of the specular behavior of water surfaces. However, Sentinel-1 alone is not sufficient for 10-day intervals and therefore where supplemented by optical data such as Sentinel-2 and Landsat-8 images. Together the sensors resulted in an average data gap of below 5% which seems satisfactory for the very cloud prone Mekong Delta.

Flood mapping using high temporal and spatial resolution based time series can contribute to flooding mitigation and adaptation in terms of water resources and coastal management. The methodology developed in this study for the Mekong Delta can be applied in similar areas at global levels such as Ganges/Brahmaputra delta in Bangladesh/ India, Niger Delta in Western Africa or Irrawaddy Delta or Ayeyarwady Delta in Myanmar.

References

[1] Le A T, Chu T H, Miller F and Bach T S 2007 Chapter 1: Flood and salinity management in the Mekong Delta, *Vietnam Challenges to Sustain. Dev. Mekong delta Reg. Natl. policy issues* Res. needs 15–68

[2] Safarzyńska K, Brouwer R and Hofkes M 2013 Evolutionary modelling of the macro-economic impacts of catastrophic flood events *Ecol. Econ.* **88** 108–118

[3] Ten Brinke W B M, Knoop J, Muilwijk H and Ligtvoet W 2017 Social disruption by flooding, a European perspective *Int. J. Disaster Risk Reduct.* **21** 312–322

[4] Dolman D I, Brown I F, ASnderson L O, Warner J F, Marchezini V and Santos G L P 2018 Rethinking socio-economic impact assessments of disasters: The 2015 flood in Rio Branco, Brazilian Amazon *Int. J. Disaster Risk Reduct.* **31** 212–219

[5] Green C 2010 Towards sustainable flood risk management Int. J. Disaster Risk Sci. 1 33–43

[6] Svetlana D, Radovan D and Ján D 2015 The economic impact of floods and their importance in different regions of the world with emphasis on Europe *Procedia Econ. Financ.* 34 649–655

[7] Talbot C J 2018 The impact of flooding on aquatic ecosystem services *Biogeochemistry*. **141** 439–461

[8] Le A T 2009 Flood risk reduction and climate change response to rice production in the Mekong Delta of Vietnam *Can Tho Univ.* J. 1–13

[9] MONRE 2016 Climate change and sea level rises scenario for Vietnam

[10] Martinis S 2010 Automatic near real-time flood detection in high resolution X-band synthetic aperture radar satellite data using context-based classification on irregular graphs (Doctor thesis) Ludwig-Maximilians-Universität München

[11] Sakamoto T, Nguyen V N, Kotera A, Ohno H, Ishitsuka N and Yokozawa M 2007 Detecting temporal changes in the extent of annual flooding within the Cambodia and the Vietnamese Mekong Delta from MODIS time-series imagery *Remote Sens. Environ*. **109** 295–313
[12] Denis G, Boissezon H, Hosford S, Pasco X, Montfort B, and Ranera F 2016 The evolution of Earth Observation satellites in Europe and its impact on the performance of emergency response services *Acta Astronaut*. **127** 619–633
[13] Brivio P A, Colombo R, Maggi M and Tomasoni R 2002 Integration of remote sensing data and GIS for accurate mapping of flooded areas *Int. J. Remote Sens*. **23** 429–441
[14] Kiage L M, Walker N D, Balasubramanian S, Babin A and Barras J 2005 Applications of Radarsat-1 synthetic aperture radar imagery to assess hurricane-related flooding of coastal Louisiana *Int. J. Remote Sens.* **26** 5359–5380
[15] Henry J B, Chastanet P, Fellah K and Desnos Y L 2006 Envisat multi-polarized ASAR data for flood mapping *Int. J. Remote Sens.* **27** 1921–1929
[16] Lang M W, Kasischke E S, Prince S D and Pittman K W 2008 Assessment of C-band synthetic aperture radar data for mapping and monitoring coastal plain forested wetlands in the Mid-Atlantic Region, U.S.A *Remote Sens. Environ.* **112** 4120–4130
[17] Mason D C, Speck R, Devereux B Schumann G J B, Neal J C and Bates P D 2010 Flood detection in urban areas using TerraSAR-X Ieee Trans. *Geosci. Remote Sens*. **48** 882–894
[18] Gstaiger V, Huth J, Gebhardt S, Wehrmann T and Kuenzer C 2012 Multi-sensoral and automated derivation of inundated areas using TerraSAR-X and ENVISAT ASAR data *Int. J. Remote Sens.* **33** 7291–7304
[19] Nguyen D T and Bui T L 2001 Flood monitoring of Mekong river delta,Vietnam using ERS Sar data 22nd Conf. Proc. Asian Conference on Remote Sensing 5–9
[20] Kuenzer C, Guo H, Huth J, Leinenkugel P, Li X and Dech S 2013 Flood mapping and flood dynamics of the mekong delta: ENVISAT-ASAR-WSM based time series analyses *Remote Sens.* **5** 687–715
[21] Le T B L 2013 Using MODIS satellite images for monitoring flood in the Mekong Delta in 2012 (Master thesis) Ho Chi Minh City University of Agriculture and Forestry
[22] Pham-Duc B, Prigent C and Aires F 2017 Surface water monitoring within Cambodia and the Vietnamese Mekong Delta over a year, with Sentinel-1 SAR observations *Water (Switzerland)*. **9** 1–21
[23] Clauss K, Ottinger M, Leinenkugel P and Kuenzer C 2018 Estimating rice production in the Mekong Delta, Vietnam, utilizing time series of Sentinel-1 SAR data *Int. J. Appl. Earth Obs. Geoinf.* **73** 574–585
[24] Minderhoud P S J, Coumou L, Erban L E, Middelkoop H, Stouthamer E and Addink E A 2018 The relation between land use and subsidence in the Vietnamese Mekong delta *Sci. Total Environ*. **634** 715–726
[25] General Statistic Office 2016 Mekong Delta Population in 2016 http://www.gso.gov.vn/default.aspx?tabid=714 (accessed 19.02.01)
[26] Mekong River Commission 2019 Physiography Mekong River Commission http://www.mrcmekong.org/mekong-basin/physiography/ (accessed 19.02.01)
[27] Liao K H, Le T A and Nguyen K V 2016 Urban design principles for flood resilience: Learning from the ecological wisdom of living with floods in the Vietnamese Mekong Delta *Landsc. Urban Plan*. **155** 69–78
[28] Nguyen N H 2012 Floodplain hydrology of the mekong delta, Vietnam *Hydrol. Process.* **26** 674–686
[29] Huynh T T H, Vo Q M and Le A T 2017 Using remote sensing MODIS data for monitoring the effects of drought and flood on rice farming system changes in the Vietnamese Mekong Delta